

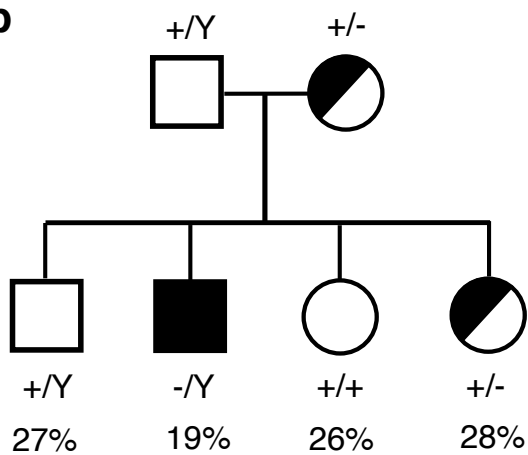
## **Chapter 5**

# **Viability and brain morphology of SAP102 mutant mice**

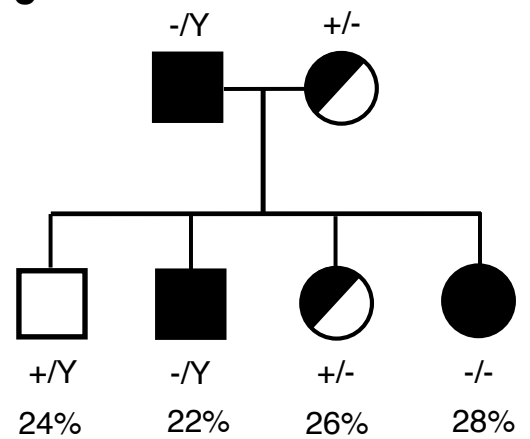
Several lines of evidence indicate roles for PSD-95 family proteins in neural development. They are expressed early postnatally during synaptogenesis and their domain structure and interaction partners suggest a potential synapse-assembly function (Funke et al., 2005). *Drosophila* dlg mutants have abnormal synapse structure (Lahey et al., 1994) and mice with a truncating mutation in SAP97 die soon after birth (Caruana and Bernstein, 2001). In contrast, synaptic structure appears normal in both PSD-95 and PSD-93 mutant mice, with a mild decrease in viability in PSD-95  $-/-$  mice but not in PSD-93  $-/-$  (McGee et al., 2001; Migaud et al., 1998). This chapter describes the characterisation of the viability, fertility and brain structure of SAP102 mutant mice.

### **5.1 SAP102 mutant mice are viable and fertile**

To examine the effect of loss of SAP102 on viability and fertility, the results of crosses between 12 heterozygous females and 4 wild-type males were analysed. These matings produced litters of approximately normal size and frequency, suggesting that the mutation does not affect female viability in the heterozygous state, although for ethical and practical reasons the equivalent wild-type litters required for a formal comparison could not be produced. Male hemizygous and female heterozygous offspring had no apparent gross abnormalities at weaning and were indistinguishable from their wild-type littermates in appearance (figure 5.1a). Figure 5.1b shows the percentage of hemizygous adult male offspring (19 %) in these litters was slightly lower than that of wild-type males (27 %), wild-type females (26 %) or heterozygous females (28 %), however a chi-squared test for goodness-of-fit indicated these proportions were not statistically different from those expected under normal mendelian inheritance ( $\chi^2 = 5.95$ ,  $n = 346$ ,  $p = 0.11$ ).

**a****b**

$n = 346$   
 $p = 0.11$

**c**

$n = 52$   
 $p = 0.95$

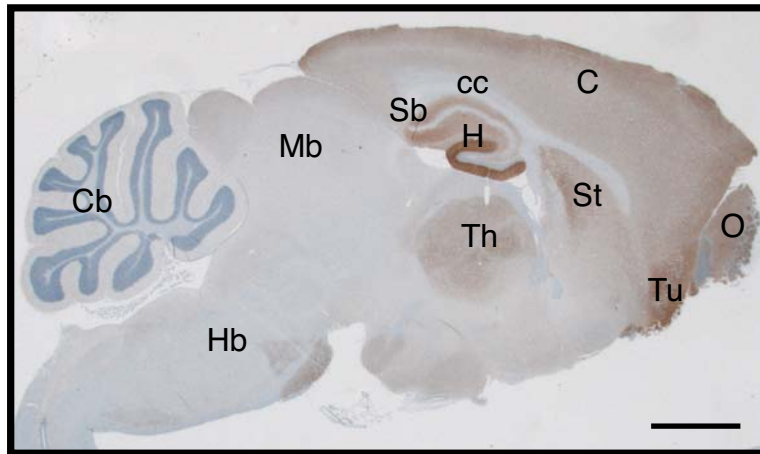
**Figure 5.1 SAP102 mutant mice are viable and fertile.** (a) Hemizygous males appear grossly normal with no obvious abnormalities. (b) Crosses between heterozygous females and wild-type males produce offspring of all expected genotypes in proportions not significantly different from those expected under mendelian inheritance ( $\chi^2 = 5.95$ ,  $n = 346$ ,  $p = 0.11$ ). (c) Crosses between hemizygous males and heterozygous females also produce mendelian ratios of the expected offspring genotypes including hemizygous males and homozygous females ( $\chi^2 = 0.37$ ,  $n = 52$ ,  $p = 0.95$ ).

Crosses between 3 hemizygous males and 6 heterozygous females also produced litters of approximately normal size and frequency, indicating no obvious effect of SAP102 loss on male fertility. Figure 5.1c shows that wild-type and hemizygous males, heterozygous and homozygous females were produced from these crosses at 24, 22, 26 and 28% respectively, proportions also no different from those expected under mendelian inheritance ( $\chi^2 = 0.37$ ,  $n = 52$ ,  $p = 0.95$ ), showing that the null mutation does not affect the survival of either male or female mice. Preliminary crosses between 2 male hemizygous and 2 female homozygous mice were also fertile, producing one litter each within 4 weeks of being placed together. The first litter consisted of 8 male and 6 female pups. The second consisted of 4 males and four females. PCR genotyping confirmed that all the male pups were hemizygous and all the females homozygous for SAP102. Thus, the SAP102 null mutation affects neither survival nor fertility in mice of either sex.

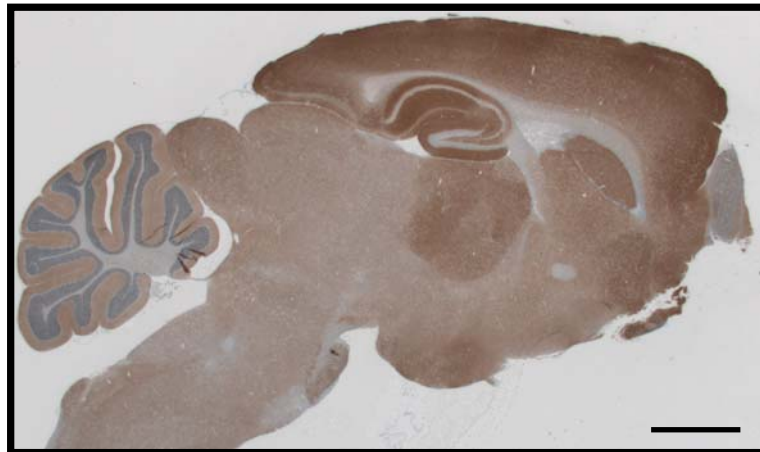
## **5.2 Expression patterns of NMDAR-associated MAGUKs in the adult mouse brain**

To inform the planned phenotypic analysis of the SAP102 mice and to search for possible differences in expression patterns between the three NMDAR-associated MAGUK proteins that could provide clues as to their differential function, an immunohistochemical study of SAP102, PSD-95 and PSD-93 expression was undertaken in the mouse brain. Four formalin-fixed, paraffin-embedded wild-type brains were sectioned parasagittally and stained separately for the three proteins of interest. Figure 5.2 shows the regional staining patterns of SAP102, PSD-95 and PSD-93 adult mouse brain (Paxinos and Franklin, 2001). The proteins display similar staining patterns with strongest expression in the hippocampus, cortex, olfactory bulb and olfactory tubercle, followed by the striatum, nucleus accumbens and pontine nuclei with the signal in remaining regions being weak or undetectable. Some regional differences were apparent, however. In the thalamus SAP102 and PSD-95 show moderate staining, while PSD-93 is weak.

SAP102



PSD-95



PSD-93

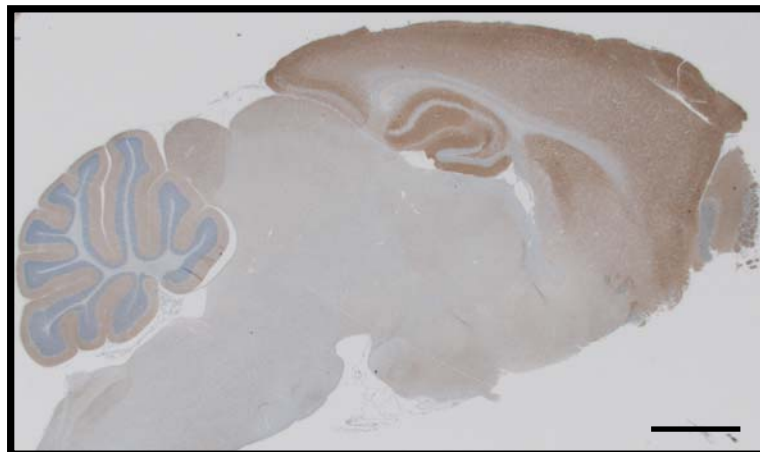


**Figure 5.2 Expression patterns of NMDAR-associated MAGUK proteins in the wild-type adult mouse brain.** Parasagittal sections are stained immunohistochemically for each MAGUK as shown (brown) and counterstained with haematoxylin (blue). C - cortex; cc - corpus callosum; H - hippocampus; St - striatum; Sb - subiculum; O - olfactory bulb; T - olfactory tubercle; Th - thalamus; Mb - midbrain; Hb - hindbrain; Cb - cerebellum. Scale bars are 2 mm.

Within the hippocampus SAP102 is strikingly stronger in the dentate gyrus than in other subregions. PSD-95 shows a mild bias towards CA1 while PSD-93 stains at approximately equal intensity in each subregion, as shown in figure 5.3a. In the cerebellum, SAP102 and PSD-95 show strong staining in the granular layer while PSD-93 is weak. In the molecular layer, PSD-95 and PSD-93 display moderate staining, with only weak signal from SAP102. SAP102 and PSD-95 are undetectable in Purkinje cells while PSD-93 is strongly expressed (figure 5.3b).

At a subcellular level, the three MAGUKs were undetectable in cell bodies throughout the brain (see figures 5.3, 5.5 and 5.6). Staining was also weak or undetectable in fibre tracts such as the corpus callosum, anterior commissure and cerebellar white matter (figure 5.2). All three MAGUKs display striated staining patterns in the dendritic layers of the hippocampus and cortex (figures 5.3a and 5.6). These staining patterns are consistent with those previously reported (Fukaya et al., 1999; Fukaya and Watabe, 2000) and with their synaptic localisation. Table 5.1 summarises the regional expression levels of the three MAGUKs.

### **5.3 Brain morphology and postsynaptic protein expression in SAP102 mutant mice**

The brain structure of SAP102 targeted mice was examined using histochemical and immunohistochemical staining of parasagittal and coronal sections from formalin-fixed, paraffin-embedded adult brain samples.

#### Whole brain

Whole brain morphology was examined by staining parasagittal brain sections from hemizygous and wild-type control mice with antibodies against the postsynaptic proteins PSD-95, PSD-93, NR1, NR2A, NR2B and MAP2B as shown in figure 5.4. Like the NMDAR-associated MAGUKs and consistent with published data (Watanabe et al., 1998; Wenzel et al., 1995), NMDAR

**Table 5.1 Regional expression patterns of NMDAR-associated MAGUK proteins in the adult mouse brain**

<u>Structure</u>			<u>Expression level</u>		
			<u>SAP102</u>	<u>PSD-95</u>	<u>PSD-93</u>
hippocampus	dentate gyrus	granular layer	-	*	*
		molecular layer	*****	***	***
		lacunosum moleculare layer	**	***	**
		polymorph layer	**	**	**
	stratum radiatum	***	***	***	
	pyramidal cell layer	-	*	*	
	stratum oriens	***	***	***	
	stratum lucidum	**	**	**	
cerebellum	white matter		-	*	-
	granular layer		***	***	*
	purkinje layer		-	-	***
	molecular layer		*	**	**
Subiculum		**	**	*	
fimbria		-	*	*	
thalamus		**	**	*	
caudate putamen (striatum)		**	**	***	
nucleus accumbens		**	**	**	
olfactory bulb		***	***	**	
olfactory tubercle		***	***	**	
cortex		***	***	***	
inferior colliculus		**	*	*	
superior colliculus		**	*	*	
hindbrain		*	*	*	
midbrain		*	*	*	
corpus callosum		-	*	*	
anterior commissure		-	*	-	

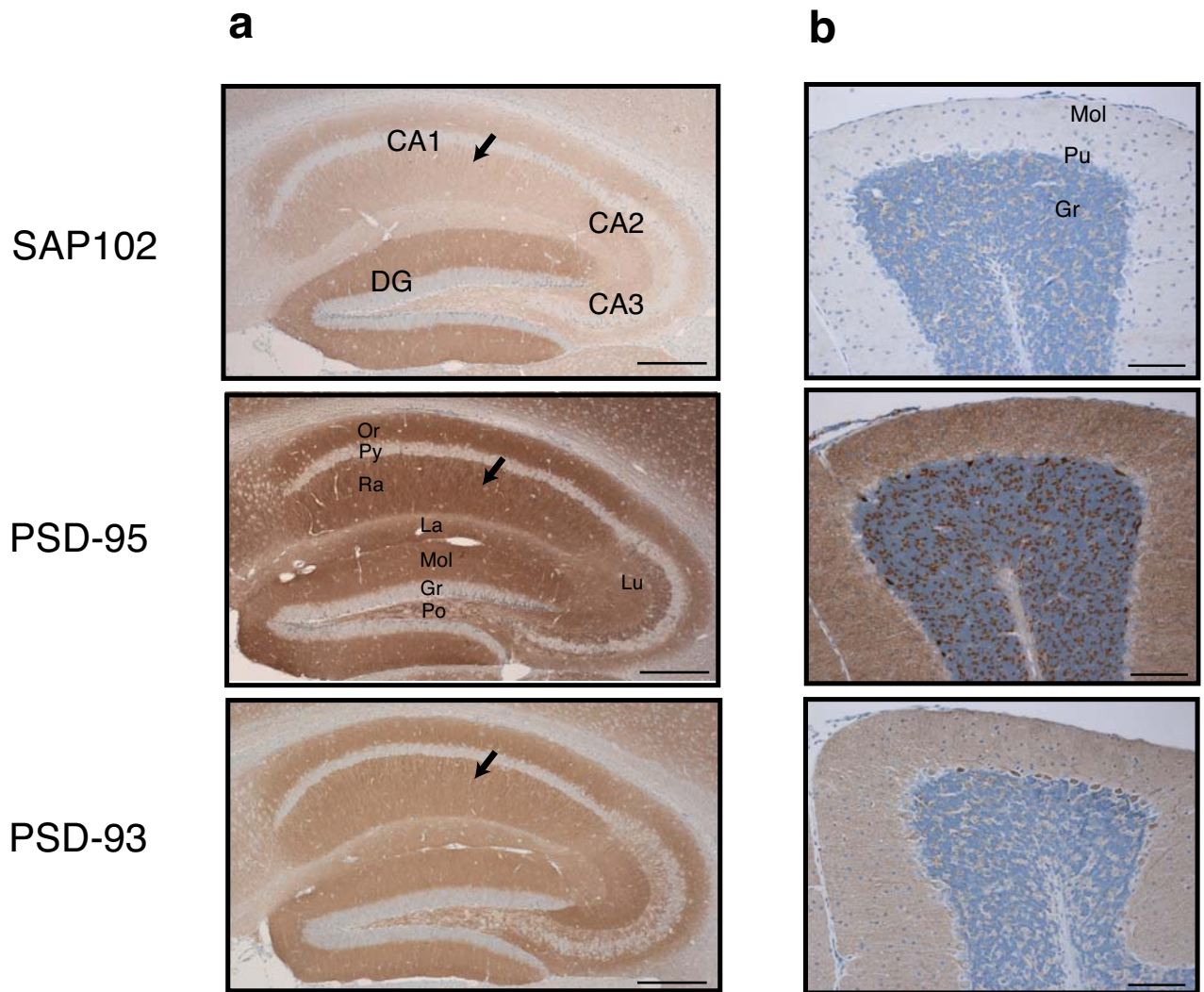


**Figure 5.3 Subregional expression patterns of NMDAR-associated MAGUK proteins in the adult mouse brain.** Parasagittal sections are stained immunohistochemically for each MAGUK as shown (brown) and counterstained with haemotoxylin (blue). **(a)** hippocampus, **(b)** cerebellum. DG - dentate gyrus; Or - stratum oriens; Py - pyramidal cell layer; Ra - stratum radiatum; La - lacunosum moleculare layer; Mol - molecular layer; Gr - granular layer; Po - polymorph layer; Lu - stratum lucidum, Pu - Purkinje cell layer. Arrow heads in (a) indicate striated dendritic staining patterns. Scale bars: (a) 500  $\mu$ m, (b) 100  $\mu$ m.



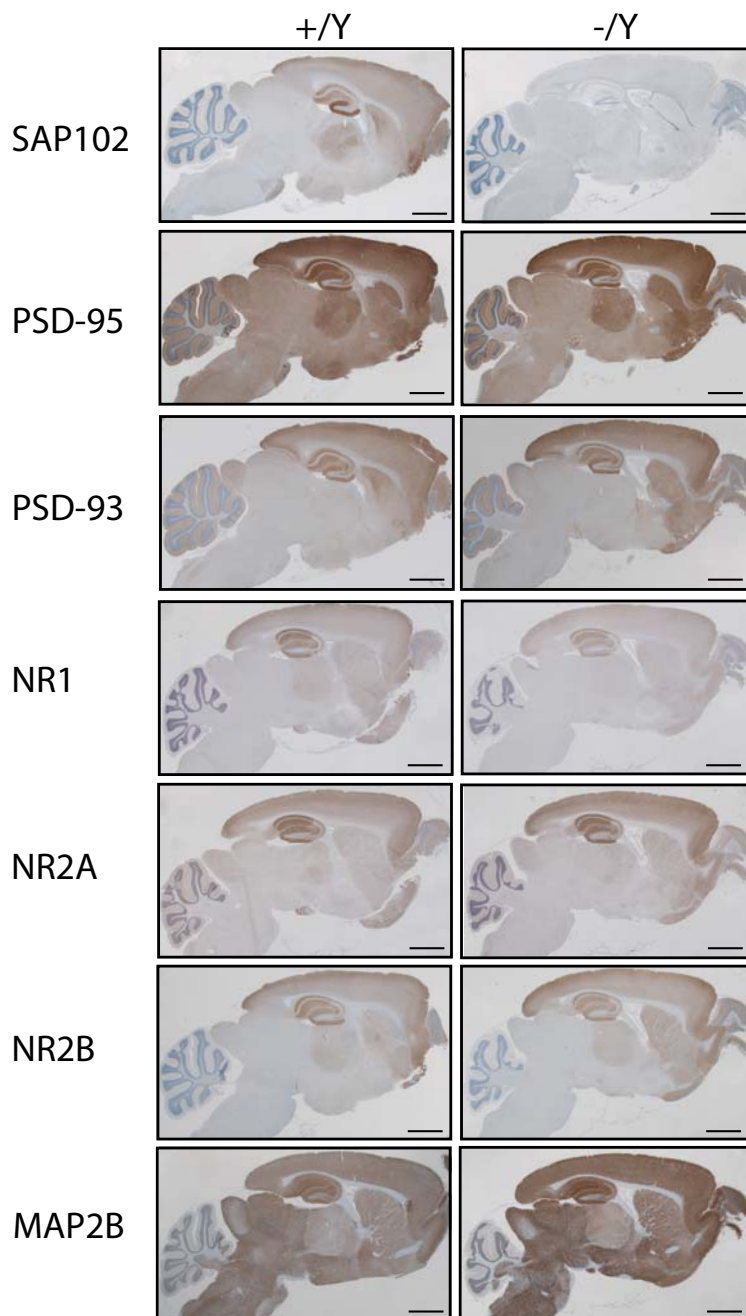


**Figure 5.4 Brain morphology and postsynaptic protein expression patterns are normal in SAP102 mutant mice.** Morphology and postsynaptic expression patterns in wild-type and SAP102 hemizygous mice in whole brain. Parasagittal sections are stained immunohistochemically (brown) as indicated and counterstained with haematoxylin (blue). Scale bars are 2 mm.

subunits exhibited strong staining in the hippocampus, cortex and olfactory bulb in both mutant and wild-type sections. Microtubule-associated protein 2B (MAP2B), a dendritic marker (Huber and Matus, 1984), produced robust staining in dendrites throughout the brain. No alterations in levels of expression or regional distributions of these proteins was observed between mutant and wild-type sections.

### Hippocampus

To examine more closely the structure of the hippocampus in SAP102 mutant mice, higher-magnification images of the region were captured as shown in figure 5.5a. In addition to the immunohistochemical stains used above, coronal sections were stained with Nissl, a cell-body stain. Hippocampal morphology appeared normal with no detectable differences between wild-type and control sections and no changes in postsynaptic protein expression levels or distribution were observed under any of the immunohistochemical stains.

Hippocampal expression levels of postsynaptic proteins were also analysed by western blot, using antibodies against the PSD-95 family proteins SAP97, PSD-95 and PSD-93, the NMDAR subunits NR1, NR2A and NR2B, the voltage-gated potassium channel Kv1.4, the AMPAR subunits GluR1 and GluR2, the kainate receptors GluR6/7, the neuregulin receptor ErbB4 and intracellular MAGUK-interacting signalling proteins SynGAP, Sec8, Pyk2, Kalirin-7 and Stargazin. Figure 5.5b shows that no differences in expression levels in these proteins were observed between hippocampal protein extracts from SAP102 hemizygous and wild-type mice.

The ultrastructure of the hippocampus was then examined using high-power light microscopy in the CA1 area. SAP102 immunohistochemical staining confirmed that even at high magnification no protein could be detected in mutant sections (figure 5.6, top panel). Despite the loss of SAP102, however, no differences were observed in the morphology or density of cell bodies in

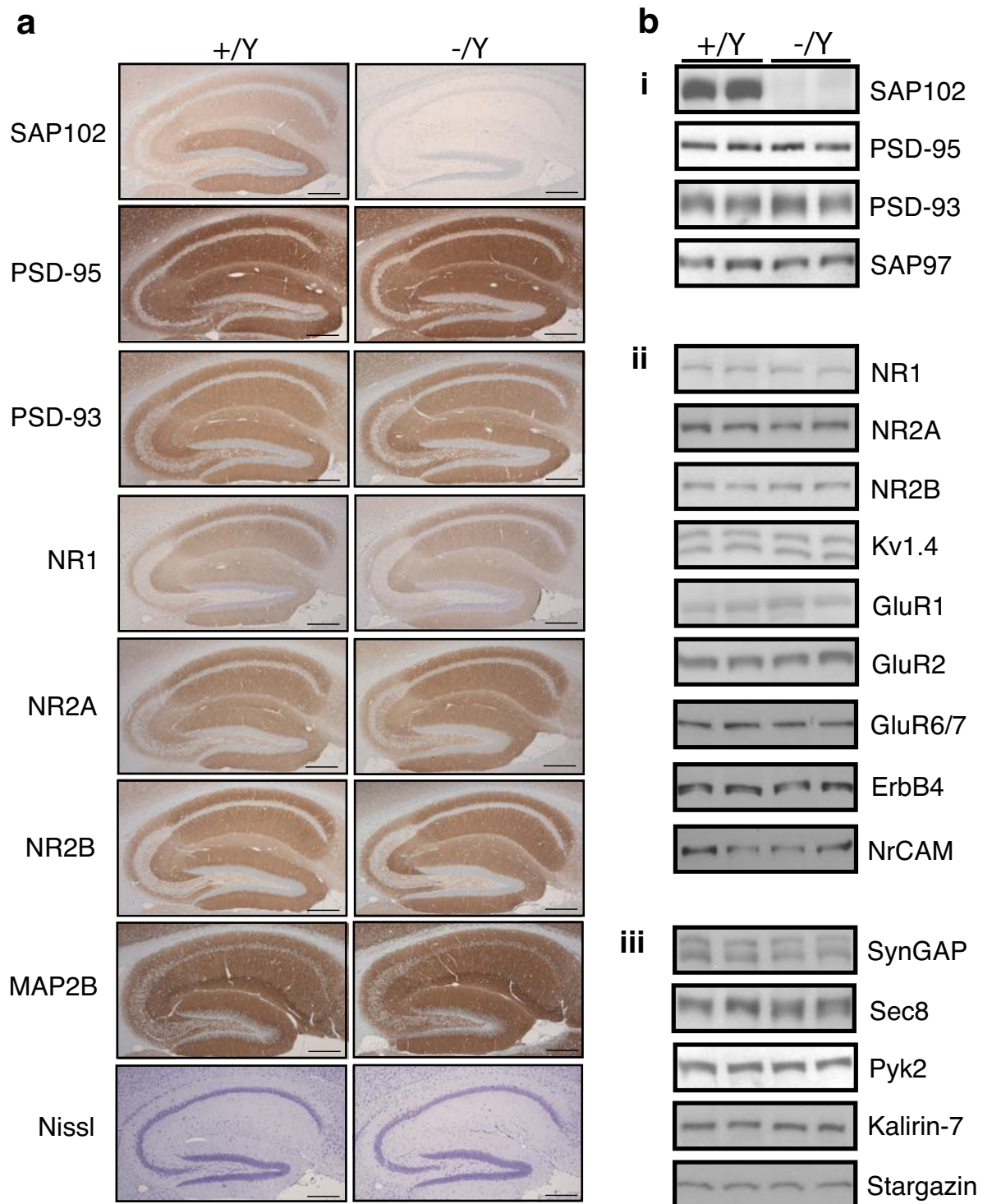


**Figure 5.5 Hippocampal morphology and postsynaptic protein expression are normal in SAP102 mutant mice.** (a) Morphology and postsynaptic expression patterns in the hippocampus of wild-type and SAP102 hemizygous mice. Parasagittal sections are stained immunohistochemically (brown) and counterstained with haematoxylin (blue) or stained with cresyl violet (Nissl) only as indicated. Scale bars are 500  $\mu$ m. (b) Normal levels of postsynaptic protein expression in the hippocampus of SAP102 mutant mice. Shown are western blots of hippocampal protein extracts for (i) PSD-95 family MAGUKs, (ii) transmembrane proteins and (iii) intracellular MAGUK-interacting proteins.

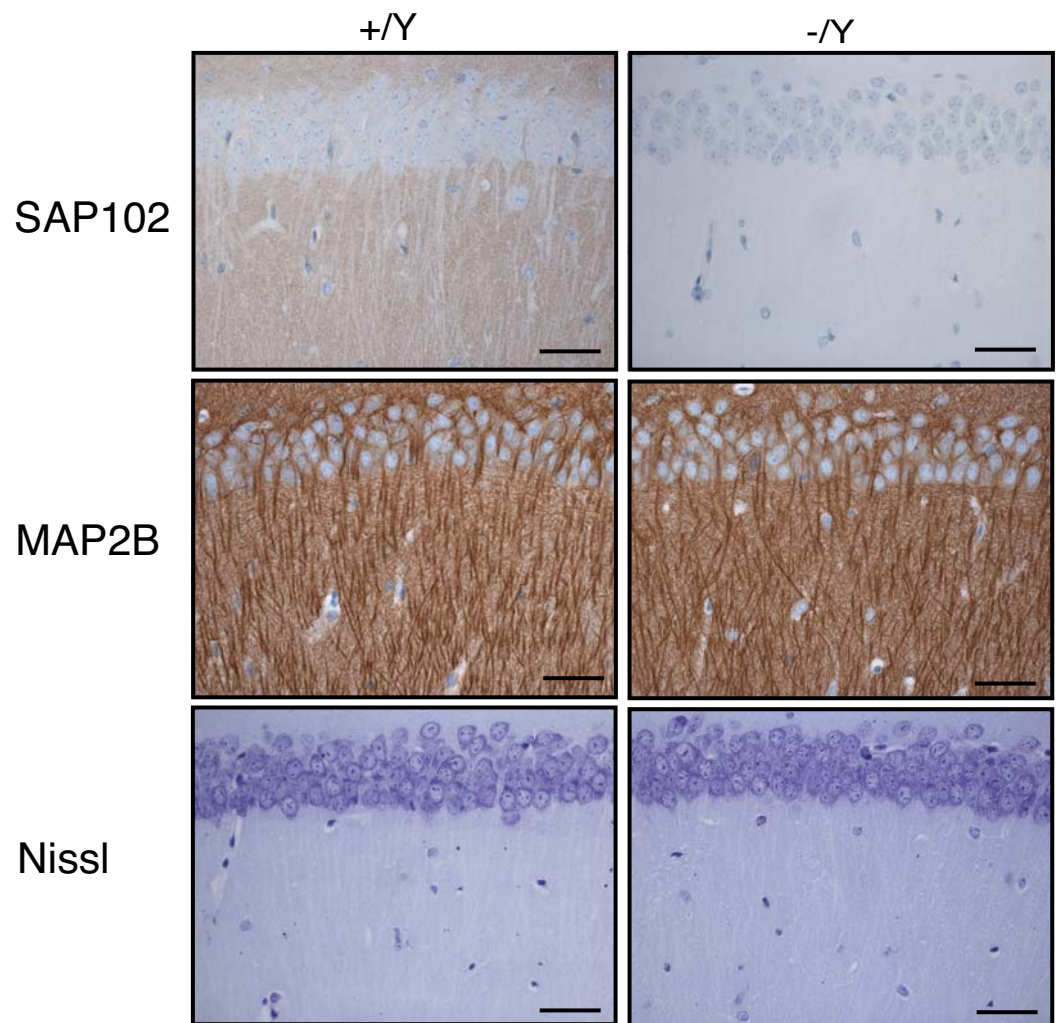


**Figure 5.6 Normal hippocampal morphology under high magnification in SAP102 mutant mice.** Sections show the CA1 pyramidal cell layer with the dendritic stratum radiatum layer below. No SAP102 staining is detectable in hemizygous brain sections even at high magnification, however dendrites stained with MAP2B and cell bodies stained with Nissl appear normal. SAP102 and MAP2B sections are counterstained with haematoxylin. Scale bars are 50  $\mu\text{m}$ .

the CA1 pyramidal area or dendrites in stratum radiatum when stained with Nissl or MAP2B respectively (figure 5.6, middle and lower panels). Finally, neuronal cell density in the hippocampus was quantified by counting columns of Nissl-stained cell bodies in pyramidal layer of CA1 and the granular layer of the dentate gyrus, shown in figure 5.7. No significant differences in mean cell density between wild-type and SAP102 mutant mice were observed in either region.

#### **5.4 SAP102 mutant mice experience a postnatal developmental delay**

In humans truncating SAP102 mutations cause developmental cognitive delay (Tarpey et al., 2004). To see if the same effect was observed in mice lacking SAP102, offspring born from matings between SAP102 heterozygous females and wild-type males were weighed every day from birth to postnatal day 14 (P14) and then every six days from P18 to P48. This experiment was performed by Lianne Stanford, Hayley Cooke and Margaret Green (Wellcome Trust Sanger Institute). Male and female pups increased in weight from approximately 1 g on the day of their birth to 9-10 g at P10 after which the sexes diverged, with males reaching 23-25 g and females 17-18 g by P48 (figure 5.8).

Analysis of body weight development of hemizygous versus wild-type male pups revealed a significant difference over the first 10 postnatal days [ $F(1, 22) = 5.98, p = 0.023$ ] but not over the entire developmental period from P1 to P48 [ $F(1, 33) = 1.29, p = 0.26$ ], as shown in figures 5.8a and 5.8c. Amongst female pups there was no significant difference in the body weights of heterozygous and wild-type individuals either during the first two postnatal weeks [ $F(1, 32) = 0.25, p = 0.62$ ] or over the entire period [ $F(1, 43) = 0.05, p = 0.83$ ], as shown in figures 5.8b and 5.8d.

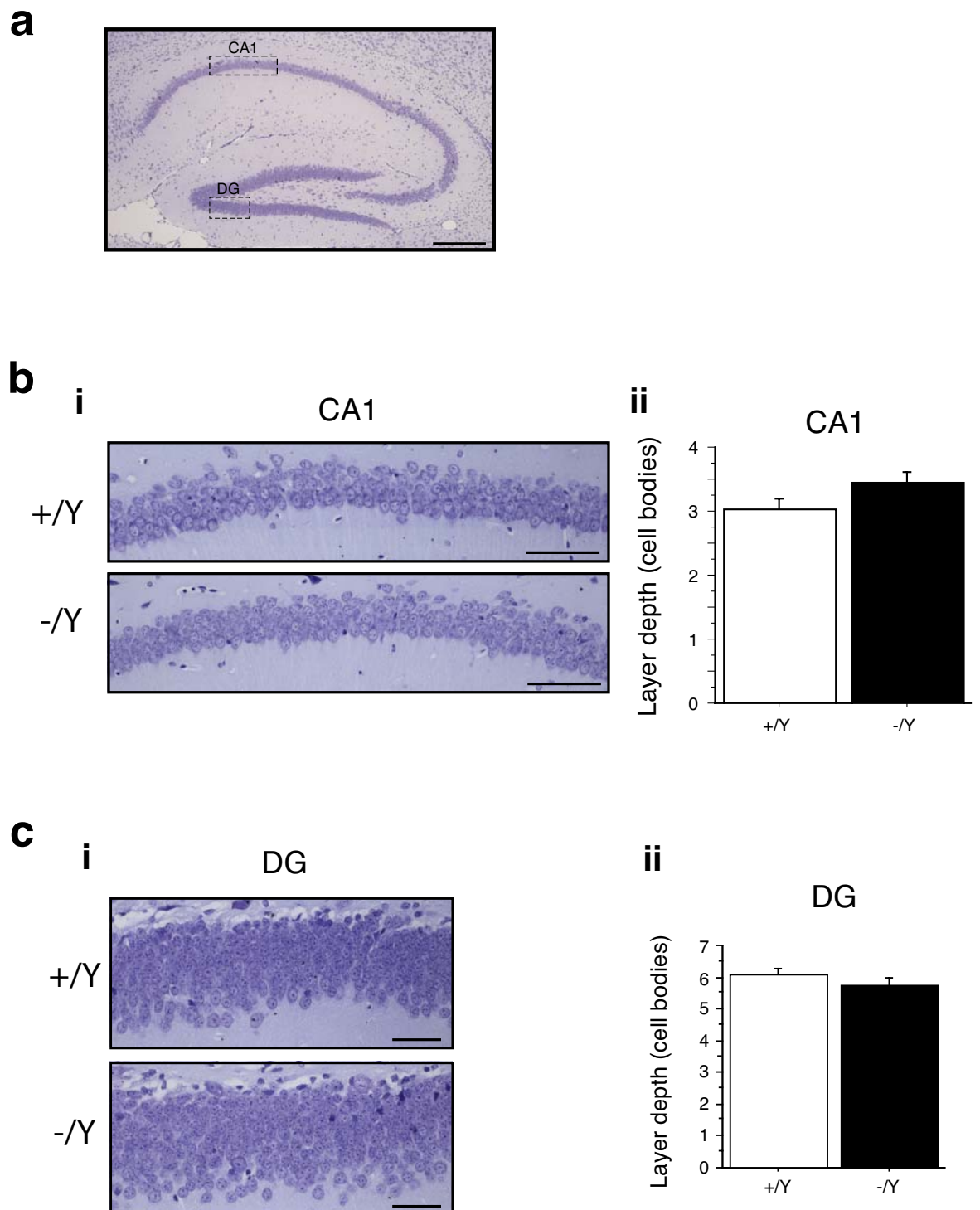


**Fig 5.7 Loss of SAP102 does not affect hippocampal cell density.** (a) Dashed rectangles indicate regions of CA1 and dentate gyrus (DG) in which cell numbers were quantified. Scale bar: 500  $\mu$ m. (b) Cell numbers in CA1. (i) Cells were quantified by counting the number of Nissl-stained cell bodies between the dorsal and ventral boundaries of the CA1 pyramidal layer at 50  $\mu$ m-intervals along the most dorsal part of the layer. Representative sections are shown. Scale bars: 100  $\mu$ m. (ii) No difference in cell numbers were observed between wild-type and hemizygous animals [ $F(1,4) = 1.23$ ,  $p = 0.33$ ]. (c) Cell numbers in the dentate gyrus. (i) Cells were quantified using the same counting method at the caudal end of the lower arm of the pyramidal layer of the dentate gyrus. Scale bars: 50  $\mu$ m. (ii) No difference between wild-type and hemizygous cell numbers was observed [ $F(1,4) = 0.36$ ,  $p = 0.58$ ].

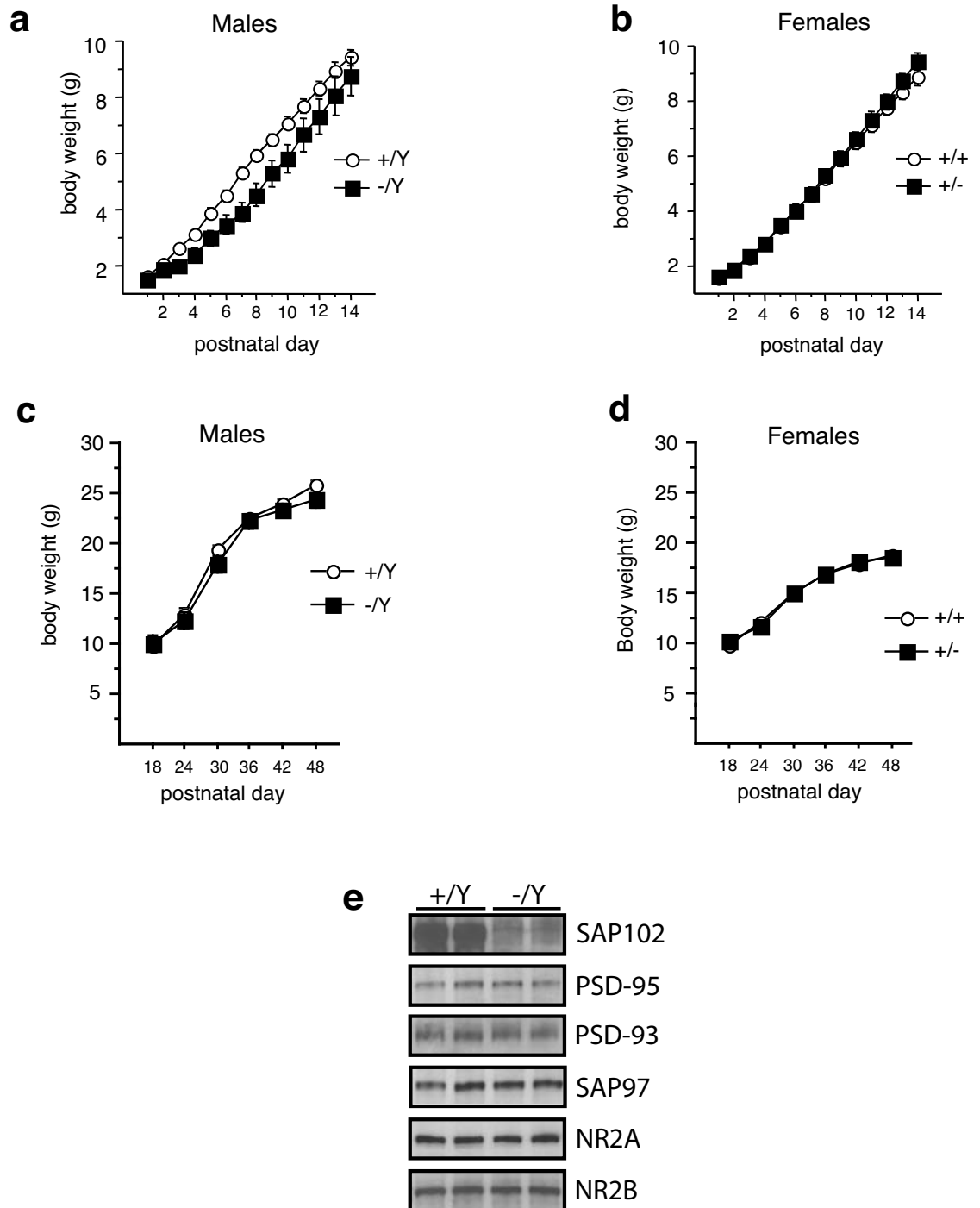


**Figure 5.8 Loss of SAP102 causes developmental delay.** (a) Body weights of male hemizygous and wild-type pups from postnatal day 1 (P1) to P14. Statistical analysis shows a significant effect of genotype on body weight [ $F(1, 22) = 5.98, p = 0.023$ ]. (b) Body weights of heterozygous females remain normal throughout the first two postnatal weeks [ $F(1, 32) = 0.25, p = 0.62$ ]. (c) No differences in body weight between wild-type and hemizygous male mice are observed between P18 and P48. Statistical analysis of body weights over the entire developmental period (P1-48) showed no effect of genotype [ $F(1, 33) = 1.29, p = 0.26$ ]. (d) No differences in body weight between wild-type and heterozygous female mice are observed between P8 and P48 [ $F(1, 43) = 0.05, p = 0.83$  for P1-48]. (e) Expression of MAGUKs and NMDA receptor subunits at P6 in the hippocampus of SAP102 mutant mice. All four MAGUKs as well as NR2A and NR2B are present and no changes in expression are observed as a result of the mutation.

Figure 5.8a shows that the weight of SAP102 <sup>-/-</sup> pups diverges after P2 and remains below that of wild-type controls until regaining parity after P12. Published data of temporal expression patterns in the mouse suggest that SAP102 is robustly expressed from P2, while PSD-95 and PSD-93 levels are almost undetectable until their expression increases around P11 (Sans et al., 2000). This provides a possible reason for the requirement of SAP102 for normal development during this period, since no other MAGUK would be available to compensate for its function. The absence of all three MAGUKs during early development in SAP102 mutant mice would also provide a valuable opportunity to test the necessity of these proteins for NMDA receptor localisation and function during this period. To examine this possibility directly, MAGUK expression was analysed using western blots of protein extracts from forebrains of wild-type and SAP102 hemizygous male mice at P6 (figure 5.8e). Surprisingly, all four MAGUK proteins were present, although PSD-95 and PSD-93 appeared to be at lower levels than in adult tissue. No changes in MAGUK levels or NMDAR subunit expression was observed as a result of SAP102 mutation at this developmental time point.

## 5.5 Discussion

SAP102, PSD-95 and PSD-93, the three NMDAR-associated MAGUK proteins, display similar regional expression patterns in the adult mouse brain with strongest expression in the hippocampus, cortex and olfactory bulb. They are absent from neuronal cell bodies but strongly stain dendritic layers where they exhibit a distinctive striated pattern, suggesting they are preferentially localised to dendritic spines and present only at low levels or are absent from dendritic shafts. These results are consistent with their known enrichment in PSD fractions (Brenman et al., 1998; Cho et al., 1992; Muller et al., 1996), their postsynaptic localisation in electron microscopic studies (Aoki et al., 2001; Roche et al., 1999; Sans et al., 2000) and previously published immunohistochemical data (Fukaya and Watabe, 2000). These regional and



subcellular staining patterns match well with those observed for their associated NMDAR subunits NR1, NR2A and NR2B.

Despite broad similarities, some differences in expression patterns are apparent and may be used to make predictions as to the differential functions of individual NMDAR-associated MAGUKs. Perhaps the most striking difference is the strong expression of SAP102 in the dendritic layer of the dentate gyrus, contrasting with PSD-95's preference for CA1. It seems likely that any disruption of synaptic plasticity in SAP102 knockout mice will be most prominent in the dentate gyrus, while the disruption in PSD-95 mutants should be strongest in CA1.

Loss of SAP102 has no apparent effect on the survival, appearance or fertility of male or female constitutively targeted mice, so a full phenotypic analysis of the consequences of germline SAP102 loss upon adulthood should be possible. This is consistent with the human disorder, in which male hemizygous and female heterozygous individuals live to adulthood and can be fertile (Tarpey et al., 2004).

Neither does the SAP102 null mutation have any observable effect upon brain morphology or postsynaptic protein expression. Whole brain sections appear structurally normal when examined under light microscopy with immunohistochemical staining, as does the general morphology and ultrastructure of the hippocampus. Hippocampal neuronal cell density is also normal and there is no evidence of disruption to expression levels or distribution patterns of postsynaptic proteins in the hippocampus either by immunohistochemical staining or western blot. Normal localisation of NMDAR subunits to hippocampal dendrites in these brain sections indicates that SAP102 may not be required for transport of this receptor to the synapse.

This result is encouraging with respect to human mental retardation, since therapeutically it is likely to be easier to compensate for an acute lack of adult SAP102 function in specific postsynaptic signalling pathways than to repair a gross structural dysmorphology. This does not preclude, however, the possibility of microscopic disruption to dendritic spine morphology which is a common mental retardation phenotype both in humans and mouse models (Comery et al., 1997; Kaufmann and Moers, 2000; Ropers and Hamel, 2005) and which could not be detected without more sophisticated microscopic techniques than have been employed here.

Loss of SAP102 does result in a postnatal developmental delay in growth from P2 to P11, corresponding closely with the period when, according to published data, SAP102 expression is strong while PSD-95 and PSD-93 expression is weak (Sans et al., 2000). Western blots showed however, that the latter two proteins were easily detectable at P6. Loss of SAP102 could cause delayed growth via several potential mechanisms. For example, impaired suckling ability could arise from lack of motor coordination as a result of cerebellar SAP102 loss. Alternatively SAP102 deficiency in the olfactory bulb could lead to olfactory impairment and a concomitant inability of a pup to find its siblings and mother for warmth and food.